

Synergies or trade-offs between surface urban heat island and hot extreme: Distinct responses in urban environments



Chen Yang^a, Shuqing Zhao^{b,*}

^a College of Urban and Environmental Sciences, Peking University, Beijing 100871, China

^b College of Ecology and the Environment, Hainan University, Haikou 570228, China

ARTICLE INFO

Keywords:

Heatwave
Urban heat island
Surface energy balance
Surface biophysical drivers
Chinese cities

ABSTRACT

Hot extremes are among the most damaging climate extremes to human society, with urban areas being particularly vulnerable due to the surface urban heat island (SUHI). Despite the growing frequency and intensity of surface hot extreme (SHX), a comprehensive understanding of the patterns and drivers of SUHI responsiveness to SHX (difference in SUHI intensity [δ SUHII] between SHX and non-hot extreme conditions [NSHX]) remains obscure. This study aims to shed light on the spatial-temporal pattern of SHX and the distinct SUHI responses to SHX throughout climatically diverse Chinese urban clusters using the seamless daily land surface temperature (LST) dataset. Our results provided evidence that Chinese urban clusters have experienced increasingly frequent, prolonged, and intensive SHX events regardless of climatic context, with stronger occurrences in summer and fall. Spatially, urban clusters in the northern regions have been subjected to more intensified SHX episodes compared to their southern counterparts. Furthermore, our findings revealed distinct δ SUHII responses to SHX across China, demonstrating synergies between SUHI and SHX when SHX events constrained to urban areas whereas trade-offs when SHX isolated within rural settings. The magnitude of δ SUHII depended upon the relative intensity of SHX between urban and rural settings, and heightened δ SUHII generally associated with more intensified SHX events in urban than rural areas. Additionally, the explainable machine learning-based driver exploration showed that δ SUHII was largely controlled by disparities in evaporative cooling (δ ET) between SHX and NSHX during the daytime, whereas during nighttime, it was predominantly governed by changes in surface heat storage, including urban-rural disparities in surface albedo (δ ABD) and impervious surface fraction (ISF). Facing the intertwined challenges posed by climate change and urbanization, it is imperative for cities to develop effective cooling strategies that emphasize enhanced evaporative cooling and minimized heat storage. These strategies are essential for safeguarding urban residents from potential synergistic effects between SUHI and SHX towards sustainable cities and human settlements.

1. Introduction

Hot extreme has become more frequent and intensified in recent years due to the continuing global warming trend (Easterling et al. 2000; Meehl and Tebaldi 2004; Sun et al. 2014). Simultaneously, the Earth is becoming an increasingly 'urbanized' planet (Angel et al. 2011; United Nations 2018). Urbanization, with its significant alterations to land surface processes that impact the surface energy balance (SEB), has given rise to the phenomenon known as the urban heat island (UHI) (Grimmond 2007; Oke 1973; Zhao et al. 2014; Zhou et al. 2014). Nowadays, extreme hots has been regarded as one of the deadliest climate extremes, causing widespread disruption to human communities

and natural ecosystems across continents (Bi et al. 2023; Gao et al. 2023; Mishra et al. 2015; Mora et al. 2017; Nangombe et al. 2018; Yin et al. 2023). UHI also significantly impacts ecosystem health (Melaas et al. 2016; Zhao et al. 2016) and human well-being (Hsu et al. 2021; Rydin et al. 2012) at the same time. Generally, numerous cities are now confronted with the dual challenges of increasing surface heat extremes (SHX) and UHI effects amidst the backdrop of ongoing climate change and urbanization.

On top of that, it is imperative to investigate whether the UHI is exacerbated during episodes of surface hot extremes. Due to the presence of the UHI, urban areas are arguably more susceptible to hot extremes compared to their rural counterparts. Even under non-surface hot

* Corresponding author.

E-mail address: shuqing.zhao@hainanu.edu.cn (S. Zhao).

extreme (NSHX) conditions, urban areas typically exhibit higher temperatures than rural backgrounds (Anderson and Bell 2009; Grimmond 2007). Potential synergies between SHX and UHI can disproportionately intensify the adverse consequences of urban overheating (He et al. 2021; Jiang et al. 2019; Li and Bou-Zeid 2013; Li et al. 2016; Li et al. 2015; Miao et al. 2022; Tan et al. 2010). Over Chinese cities located in humid and arid climates, Miao et al. (2022) have found that surface UHI (SUHI) intensity is augmented by hot extremes, especially in the north subtropical climate (SUHI intensified by 0.72 ± 0.54 K for daytime and 0.29 ± 0.23 K for the nighttime). Observational evidence from Europe also demonstrates an intensification of the air Urban Heat Island (AUHI) for most cities during nighttime extreme hot events (Possega et al. 2022). Similarly, in cities across the United States with a temperate climate, SUHI and AUHI increased by 2.8°C and 0.4°C , respectively, during episodes of hot extremes (Zhao et al. 2018). The interconnections between UHI and hot extremes are not always synergetic, and UHI responses to extreme heat exhibit variability dependent on factors such as time, climatic conditions, and city scale. For instance, it is noteworthy that extreme heat tends to accentuate UHI effects in larger urban areas (e.g., New York and Washington), while smaller cities show no observable UHI augmentation (Ramamurthy and Bou-Zeid 2017). Additionally, when experiencing episodes of extreme heat, the daytime and nighttime UHI in cities such as Beijing and Shanghai demonstrate an augmentation compared to non-extreme hot conditions (Jiang et al. 2019). In contrast, the daytime UHI in Guangzhou exhibits a moderating trend during extreme heat events, leading to a slight alleviation of approximately 0.2°C (Jiang et al. 2019). This nuanced behavior underscores the importance of considering various contextual factors when analyzing UHI responses to extreme heat.

However, the interactions between UHI and hot extremes, as well as the intricate contextual dependencies and the potential drivers of the varying UHI patterns during hot extreme episodes remain incompletely deciphered. The complexity arises from the heterogeneity in research focus, whether it pertains to the SUHI or AUHI, the diversity in data sources employed, and the variations in modeling and observational methodologies employed. Such diversities introduce ambiguity into our understanding of UHI responsiveness to hot extremes and raise concerns regarding the robustness of the underlying mechanistic examinations (Miao et al. 2022; Possega et al. 2022; Ward et al. 2016). Furthermore, current research lacunae underscore the need for the exploration of temperature records across multiple years rather than the examination of individual hot extreme events. There is a growing recognition of the importance of encompassing a diverse ensemble of cities, each characterized by varying natural settings and built environment properties. Such an approach is essential for unveiling the overarching responsive patterns of UHI to hot extremes (Possega et al. 2022; Wei et al. 2021). It is worth noting that a significant portion of the research endeavors aimed at unraveling the mechanisms behind the responsiveness of the Surface Urban Heat Island (SUHI) to surface hot extremes (SHX) have predominantly relied on physical models. These models are known for their computational intensity and the requirement for extensive flux data to ensure accurate simulations (Fenner et al. 2019; Founda and Santamouris 2017; Li and Bou-Zeid 2013; Li et al. 2015; Ngarambe et al. 2020). Conversely, there is a growing trend toward the adoption of statistical models to investigate the drivers of SUHI responsiveness. This preference can be attributed to their efficiency and generalizability, with interpretable machine learning techniques progressively gaining prominence in this context (Berdugo et al. 2022; Kim and Kim 2022; Miao et al. 2022; Oukawa et al. 2022; Zhou et al. 2022). Utilizing extensive, long-term time-series land surface temperature (LST) observations, this study aims to determine whether Chinese urban areas conform to the prevailing paradigm of positive responsiveness of SUHI to surface heat extremes (SHX). Moreover, it seeks to enhance our comprehension of the fundamental physical drivers underpinning the interrelationship between SUHI and SHX in Chinese urban areas encompassing a wide range of climatic conditions. This study specifically focuses on

satellite-derived SUHI, given its multifaceted significance concerning the urban thermal environment and ecosystem conditions, along with its robust and conceptually clear theoretical foundation (Manoli et al. 2019; Miao et al. 2022; Venter et al. 2021; Zhao et al. 2014; Zhao et al. 2018).

2. Materials and methods

2.1. Study area

We have selected 482 Chinese urban clusters situated within diverse climatic contexts, as illustrated in Figure S1. These clusters have remained consistent throughout the entire study duration, spanning from 2003 to 2020, and possess built-up areas exceeding 10 km^2 . These urban clusters are mainly located in seven climate zones characterized by air temperature, precipitation, and days with average daily temperatures surpassing 10°C , et al. (China National Institute of Standardization 1998; Wang et al. 2017; Zhang and Zhu 1959; Zheng et al. 2010). These seven main climates are mid-temperate (MT), south-temperate (ST), north-sub-tropical (NSTr), mid-sub-tropical (MSTr), south-sub-tropical (SSTr), north-tropical (NTr), and plateau (PLT). The spatial extent of these selected urban clusters has been delineated annually employing the city clustering algorithm (CCA) with a clustering parameter of 2 km (Rozenfeld et al. 2008). This delineation has been accomplished using data from the 1 km global annual urban extent dataset (Zhao et al. 2022). Furthermore, pixels demonstrating low imperviousness (imperviousness $< 20\%$) within the urban boundaries have been excluded, guided by the annual impervious surface (IS) map developed by Yang and Huang (2021).

2.2. Surface hot extreme (SHX) and non-surface hot extreme (NSHX) conditions definition

In this study, LST has been employed as a proxy for near-surface air temperature (NSAT) in order to define and identify episodes of SHX. The adaptation of LST is grounded in the well-documented association between LST and NSAT (Amani-Beni et al. 2022; Good et al. 2017; Wei et al. 2021). Furthermore, it aligns favorably with the guidelines established by the World Meteorological Organization (WMO) for identifying climate extremes (World Meteorological Organization 1989, 2017). To identify surface hot extremes occurrences, we employed percentile thresholds based on long-term LST data spanning from 2003 to 2020. To detect occurrences of surface hot extremes, we have employed percentile-based thresholds derived from long-term LST data spanning from 2003 to 2020. The identification of hot extremes is contingent on variables such as the threshold values for temperature extremes, the duration of hot extremes, and the selection of climatic or bioclimatic indices (Easterling et al. 2000; Meehl and Tebaldi 2004; Perkins and Alexander 2013). The use of percentile-based definitions for hot extremes offers distinct advantages when it comes to assessing and comparing SUHI responses to hot extremes across diverse climatic settings, in contrast to fixed-temperature absolute thresholds (Cheng et al. 2023; Founda and Santamouris 2017; Igun et al. 2023; Liao et al. 2021; Miao et al. 2022; Shi et al. 2021a). The surface hot extreme has been defined as a period lasting a minimum of three consecutive days during which the urban/rural average LST (i.e., LST_{urban} or LST_{rural}) exceeded the 90th percentile of the long-term LST collection, as defined by equation [1].

$$LST \text{ collection} = Year_{y=2003}^{y=2020} Date_{d=i-7}^{d=i+7} LST_{y,i} \quad (1)$$

For each day or night, the daily-based percentile has been calculated from a 15-day time window (including the specific day, the week preceding it, and the week following it) centered on each calendar day spanning from 2003 to 2020. This process has resulted in a total of daily samples, amounting to $15 \text{ days} \times 18 \text{ years}$, equating to 270 days in total.

The SHX identification has been implemented over urban areas and corresponding rural surroundings individually. Specifically, we identified four types of surface hot extremes:

1. Daytime urban hot extreme (DUHX)—at least three consecutive hot days over urban areas (i.e., the daytime $LST_{urban} > 90$ th percentile threshold).
2. Nighttime urban hot extreme (NUHX)—at least three consecutive hot nights over urban areas (i.e., the nighttime $LST_{urban} > 90$ th percentile threshold).
3. Daytime rural hot extreme (DRHX)—at least three consecutive hot days over rural surroundings (i.e., the daytime $LST_{rural} > 90$ th percentile threshold).
4. Nighttime rural hot extreme (NRHX)—at least three consecutive hot nights over rural surroundings (i.e., the nighttime $LST_{rural} > 90$ th percentile threshold).

Since SUHI is a combined output of the urban-rural dichotomy, fluctuations in both urban (LST_{urban}) and rural (LST_{rural}) LST during periods of surface hot extremes can lead to corresponding alterations in SUHI intensity when compared to non-surface hot extreme (NSHX) conditions. In order to investigate the SUHI responsiveness to SHX in further detail, each day or night in four types of surface hot extremes has been distinguished into six SHX scenarios:

1. Individual urban hot day (IUHD)—a specific day when a surface hot extreme onsets only in urban area but not in rural surroundings (i.e., $IUHD \in DUHX$ and $IUHD \notin DRHX$).
2. Individual rural hot day (IRHD)—a specific day when a surface hot extreme onsets only in rural surroundings but not in urban areas (i.e., $IUHD \notin DUHX$ and $IUHD \in DRHX$).
3. Compound hot day (CHD)—a specific day when surface hot extremes onset in both urban and rural areas (i.e., $CHD \in (DUHX \cap DRHX)$).
4. Individual urban hot night (IUHN)—a specific night when a surface hot extreme onsets only in urban area but not in rural surroundings (i.e., $IUHN \in NUHX$ and $IUHN \notin NRHX$).
5. Individual rural hot night (IRHN)—a specific night when a surface hot extreme onsets only in rural surroundings but not in urban areas (i.e., $IUHN \notin NUHX$ and $IUHN \in NRHX$).

6. Compound hot night (CHN)—a specific night when surface hot extremes onset in both urban and rural areas (i.e., $CHN \in (NUHX \cap NRHX)$).

Details on the definition of SHX and various types of hot days/nights have also been shown in Fig. 1 for better illustration. Since the seamless daily LST dataset is based on clear-sky conditions, we have introduced a weighting preprocess to improve the robustness of LST data. First, we have categorized the 1km LST observations into four levels (i.e., MODIS LST error $\leq 1^{\circ}\text{C}$, $\leq 2^{\circ}\text{C}$, $\leq 3^{\circ}\text{C}$, and $> 3^{\circ}\text{C}$) based on the quality control information in raw MODIS product. The weights w are assigned inversely proportional to each 1km LST observation, i.e., $w = \frac{1}{\text{error}^2}$. The interpolated LST observations with MODIS LST error $> 3^{\circ}\text{C}$ have been weighted as $\frac{1}{16}$, and so on. The LST_{urban} and LST_{rural} are the w -weighted arithmetic means of grid cell LST within urban areas and rural surroundings, respectively.

In addition, this study has taken into consideration three hot extreme characteristics, including frequency, duration, and amplitude (Dong et al. 2021; Perkins and Alexander 2013; Shi et al. 2021b). Surface hot extreme frequency (HXF) is the sum of the number of surface hot extreme in each year. Surface hot extreme duration (HxD, in units of days) is the total number of consecutive days that comprise a surface hot extreme (number of days of LST_{urban}/LST_{rural} exceeding the historical 90th threshold). Surface hot extreme intensity (Hxi, in units of $^{\circ}\text{C}$) is the accumulative threshold exceedance of LST_{urban}/LST_{rural} for a surface hot extreme. We have summed the HxD and Hxi of all the surface hot extremes for each year and obtained an annually resolved time series over each Chinese urban cluster. The trends of changes in HXF, HxD, and Hxi from 2003 to 2020 over each urban cluster have been estimated using the non-parametric Mann-Kendall (Mann 1945) trend test and Sen's (Sen 1968) slope method at the 0.05 significance level.

2.3. SUHI intensity and its responses to surface hot extreme (δSUHII) quantification

We have calculated the surface urban heat island intensity (SUHII) for each day spanning in 2003-2020 using a kernel-based methodology. For each urban cluster, the urban average LST (LST_{urban}) has been calculated using LST observations from the seamless 1km daily LST dataset (Zhang et al. 2022) over 1km built-up pixels within the urban

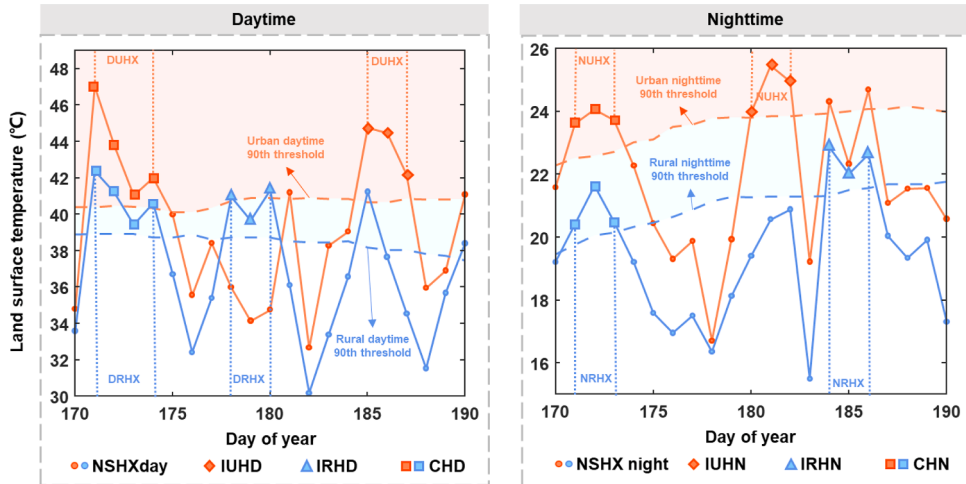


Fig. 1. Schematic definition of the surface hot extreme (SHX) over Beijing in 2003 as an example. In the figure, red and blue colors reflect land surface temperature (LST) in urban areas and rural surroundings, respectively, while dots represent non-surface hot extreme (NSHX) days or nights. A daytime/nighttime urban SHX (DUHX/DRHX) or a daytime/nighttime rural SHX (NUHX/NRHX) requires at least three consecutive days or nights above the 90th LST percentile of the long-term LST collection. Diamonds and triangles are individual urban hot days/nights (IUHD/IUHN) and individual rural hot days/nights (IRHD/IRHN). Only in the simultaneous urban and rural surface hot extreme episode (i.e., simultaneous DUHX-DRHX occurrence and simultaneous NUHX-NRHX occurrence), the corresponding day or night are recognized as a compound hot day (CHD) or a compound hot night (CHN).

extents. The rural background LST (LST_{rural}) has been calculated as the average LST of rural surroundings. The kernel-based method has dynamically determined the spatial extent of the rural surroundings around the urban cluster based on their sizes. In each year, non-urban pixels located within twice the radius of the minimum circumscribed circle (MCC) have been designated as the rural backgrounds. Water pixels, urbanized pixels (imperviousness $\geq 20\%$), and extremely elevated/low pixels (urban average elevation $\pm 50\text{m}$) have been excluded after the initial rural surroundings delineation. The SUHII can be calculated as:

$$SUHII = LST_{urban} - LST_{rural} \quad (2)$$

It is noteworthy that there are two LST observations each day in the reconstructed LST dataset, one during the daytime and one during the nighttime. Generally, the SUHII is augmented if there is a positive or synergistic interaction between surface hot extreme and SUHI. Correspondingly, it is understandable to calculate the responsive sensitivity of SUHI to SHX ($\delta SUHII$) on a daily basis as:

$$\delta SUHII = SUHII_{SHX} - SUHII_{NSHX} \quad (3)$$

$SUHII_{SHX}$ is the SUHII of a specific hot day/hot night (i.e., IUHD, IRHD, CHD, IUHN, IRHN, and CHN). $SUHII_{NSHX}$ is the average SUHII for three NSHX days/nights before and after a particular surface hot extreme. The statistical significance of $\delta SUHII$ in various climate zones has been tested using the one-sample t-test at the 0.05 significance level.

2.4. Potential drivers of SUHI responsiveness to surface hot extreme

The SUHI, in general, is induced by the perturbation of SEB by anthropogenic surface transformations in the built-up environment. These modifications encompass reduced evaporative and convective cooling processes (Li et al. 2019b; Zhou et al. 2016), increased radiative storing and trapping owing to the lower albedo (Shen et al. 2021; Shen et al. 2023; Venter et al. 2021), as well as larger heat release (Chen et al. 2022; Jin et al. 2020). Notably, significant discrepancies between Surface hot extremes (SHX) and Non-surface hot extremes (NSHX) conditions manifest in the alterations of net surface radiation and the partitioning of surface heat flux resulting from urbanization. The accessibility of key indicators of land surface properties and processes on a global scale has been greatly facilitated by advancements in reanalysis and Earth observation. Table S1 provides a comprehensive account of the potential drivers governing the responses of SUHI to SHX. It is imperative to acknowledge that the surface biophysical parameters and climatic forcings, sourced from the Global Land Data Assimilation System (GLDAS) dataset (Li et al. 2019a) do not incorporate the urban signals into the reanalysis data. Reflecting the complex processes perturbed by urban built-up characteristics through reanalysis data is challenging because even state-of-the-art Earth system models generally lack urban representation (Zheng et al. 2021). All datasets have been preprocessed on the Google Earth Engine (GEE) platform with reprojection (into the WGS84 geographic coordinate system), resampling (30 arc-seconds), and spatial extraction. The preprocessing of external variables that represent SHX-NSHX comparisons have shared the same definition of SHX and NSHX conditions with the calculation of $\delta SUHII$.

2.5. Explainable machine learning

To further decode the underlying processes and the magnitudes that potential drivers impacting SUHI responsiveness, we have adopted the eXtreme Gradient Boosting (XGBoost) regression (Chen and Guestrin, 2016), an advanced machine learning (ML) technique renowned for its ability to probe nonlinear and nonadditive relationships among features. The XGBoost model is a boosting algorithm that assembles a collection of shallow decision trees, wherein subsequent models refine the performance of prior models with reduced computational cost and enhanced

accuracy. We have developed distinct XGBoost models for each of the six distinct surface hot extreme scenarios (namely, IUHD, IRHD, CHD, IUHN, IRHN, and CHN, as detailed in Section 2.2) across all seasons. The XGBoost models have been implemented using the python package “xgboost” (Chen and Guestrin 2016), and hyperparameters in XGBoost have been tuned using the GridSearchCV algorithm the python package “sci-kit learn” (Pedregosa et al. 2011). The final XGBoost models have been trained using 70% of the complete sample dataset, comprising all specific hot days and nights under the six SHX conditions, and subsequently evaluated against the remaining 30% of independent test samples to prevent overfitting. In total, 24 XGBoost regressors have been established to address the six diverse SHX scenarios (i.e., IUHD/IUHN, IRHD/IRHN, and CHD/CHN, as outlined in Section 2.2) across all four seasons. The performance of these regressors can be referenced in Table S2.

The TreeExplainer-based SHapley Additive exPlanations (SHAP) framework has been employed to scrutinize the underlying mechanisms governing the responsiveness of SUHI to surface hot extremes (Lundberg et al. 2020). The TreeExplainer, as part of this framework, is instrumental in determining the local interpretation, specifically, how input features influence individual predictions and the interaction effects that stem from the measurement of the marginal contribution of these features. SHAP, an explanation technique in the realm of machine learning, is model-agnostic and draws its foundation from the Shapley values of game theory (Lundberg and Lee 2017). This technique directly quantifies the impact of potential drivers, as enumerated in Table S1, on the disparities between the predicted and expected values of $\delta SUHII$. It allows for a comprehensive assessment of the significance of each driver in relation to $\delta SUHII$, along with the exploration of interactions among these drivers (Lundberg et al. 2020). The SHAP value unit is $^{\circ}\text{C}$, corresponding to the unit of $\delta SUHII$.

For the convenient reference, the methodologies elucidated above have been visually presented in the subsequent technical framework.

3. Results

3.1. Patterns and dynamics in surface hot extreme characteristics across climates in China

Throughout the timeframe spanning from 2003 to 2020, surface hot extremes in China have exhibited notable latitudinal variations in intensity, denoted as HXI. This variation signifies that urban clusters in northern China have generally encountered heightened daytime and nighttime surface hot extremes when compared to their counterparts in southern regions, as visually depicted in Fig. 2. Furthermore, it is noteworthy that surface hot extremes have exhibited increased intensity during nighttime in urban clusters around the mid-latitude region (approximately 30°N). As surface hot extremes do not manifest annually, we have aggregated data encompassing the frequency, duration, and intensity of these occurrences within each urban cluster for individual years, accounting for various climate zones. The analysis has revealed a consistent pattern where urban clusters in northern China consistently grapple with more intense daytime and nighttime SHX episodes in the period spanning from 2003 to 2020, as indicated in Fig. 3. Moreover, a more substantial escalation in HXI has been observed within Chinese urban clusters situated in cooler climates, particularly within the MT, ST, and PLT climate zones, as demonstrated in Fig. 4. Irrespective of factors such as urban-rural distinctions and variations between daytime and nighttime, surface hot extreme episodes have tended to exhibit heightened intensity, increased persistence, and greater frequency during the summer season in contrast to other seasons, as illustrated in Figs. 3 and S2 and S3. Furthermore, it is worth noting that surface hot extreme episodes occurring during the daytime in China have generally manifested with greater intensity when compared to those transpiring at nighttime, exemplified by the observation that DUHX/DRHX exhibits greater intensity than NUHX/NRHX.

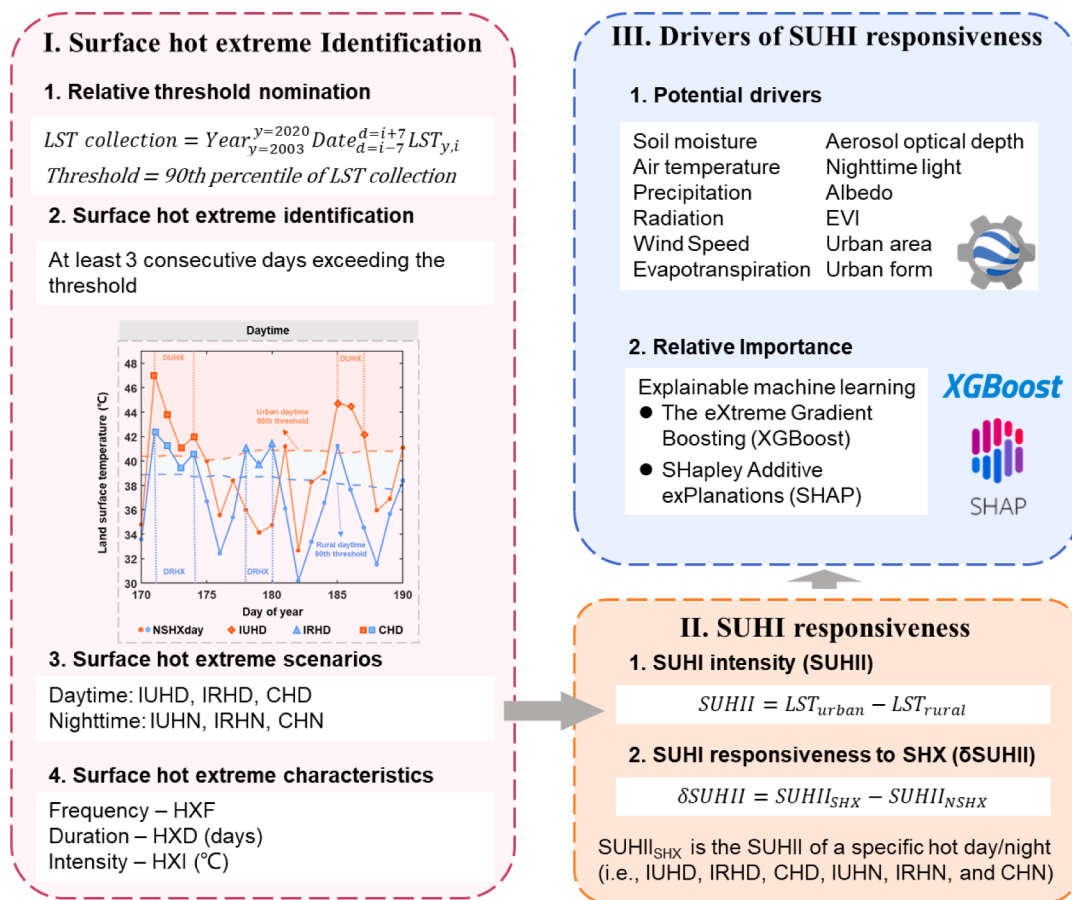


Fig. 2. The technical framework of this study.

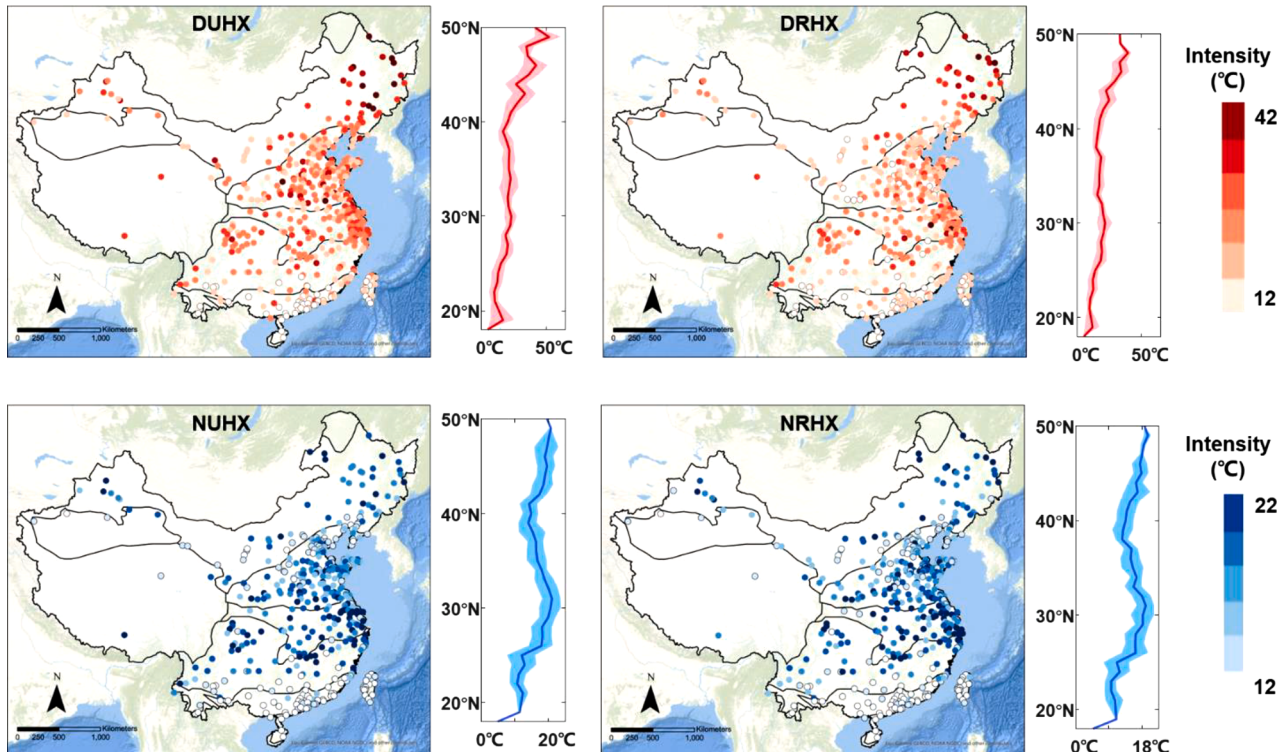


Fig. 3. The latitudinal patterns of the daytime and nighttime surface hot extreme intensity over Chinese urban clusters and corresponding rural backgrounds from 2003 to 2020. The standard deviation is shown by the shaded area.

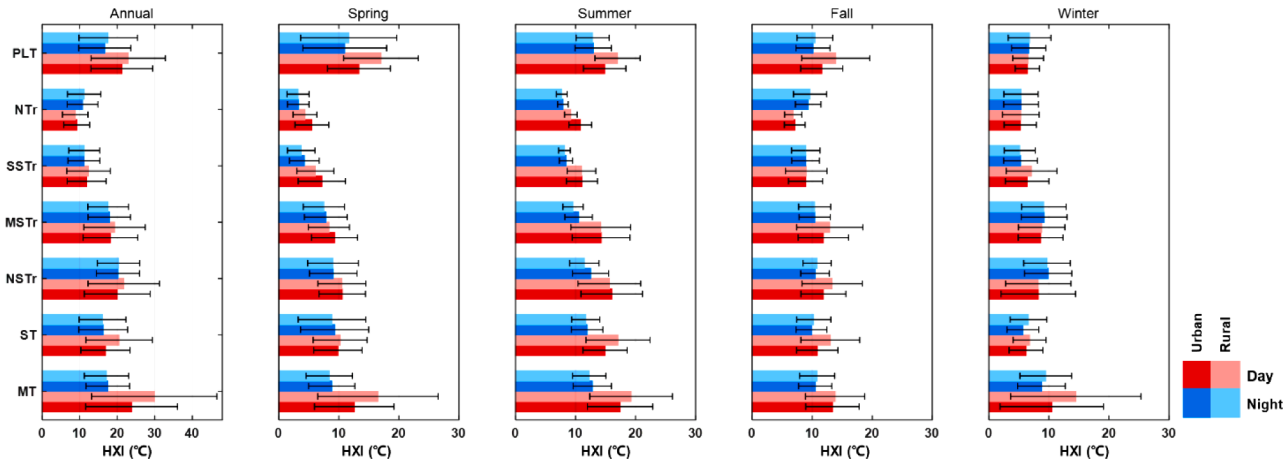


Fig. 4. The average intensity of surface hot extreme (Hxi) over urban and rural areas in the daytime (DUHX and DRHX) and nighttime (NUHX and NRHX) in various seasons and climate zones. The error bar is one standard deviation.

In each Chinese urban cluster, we have conducted Sen's slope estimation and the Mann-Kendall test on three characteristics of surface hot extremes (SHX), specifically HXI, HXD, and HXF. Moreover, we have aggregated the estimated Sen's slopes within each climate zone, encompassing only those slopes pertaining to changes in surface hot extreme characteristics that demonstrate statistical significance (p -value < 0.05). Despite the variations in climate zones, the intensity of SHX has shown statistically significant enhancement, both within urban built environments and their surrounding rural areas. As can be observed, during the past two decades, urban clusters within each climate zone have experienced more substantial increases in HXI, primarily during the summer, while experiencing comparatively fewer amplifications in spring and winter. Similarly, the modifications in the duration of surface hot extreme episodes from 2003 to 2020 have exhibited analogous seasonal patterns, as portrayed in Figure S4, with surface hot extremes during the summer persisting for more extended periods. In contrast, variations in HXF changes, both on an annual and seasonal basis, have been less pronounced, demonstrating positive trends across all seasons. Notably, despite their longer duration and increased intensity in the summer, the occurrence of summer surface hot extremes has been not inherently more frequent than in other seasons, as evidenced in Figure

S5. Furthermore, none of the three surface hot extreme characteristics have exhibited significant changes within urban clusters situated in the plateau climate zone, whether at the annual or seasonal level; hence, they have not been pooled or presented. This disparity from observations based on surface air temperature and reanalysis data (Liao et al. 2021; Luo et al. 2022; Shi et al. 2021a; Shi et al. 2021b), can likely be attributed to our specific focus on urban clusters and the corresponding scarcity of time-series data associated with urban clusters within plateau climate regions.

3.2. Responses of SUHI to surface hot extreme

Currently, a predominant consensus has yet to emerge regarding the responsiveness of the Urban Heat Island (SUHI) to surface hot extremes (SHX). Given that the SUHI phenomenon itself arises from the interplay of urban and rural dynamics, there is a compelling rationale for investigating SUHI responsiveness across diverse scenarios of urban and rural SHX episodes. As depicted in Fig. 5, the direction and magnitude of SUHI responsiveness to SHX have exhibited variations contingent upon the prevailing climate and season. Irrespective of climate or the time of year, when SHX has exclusively impacted urban areas, SUHI has registered a

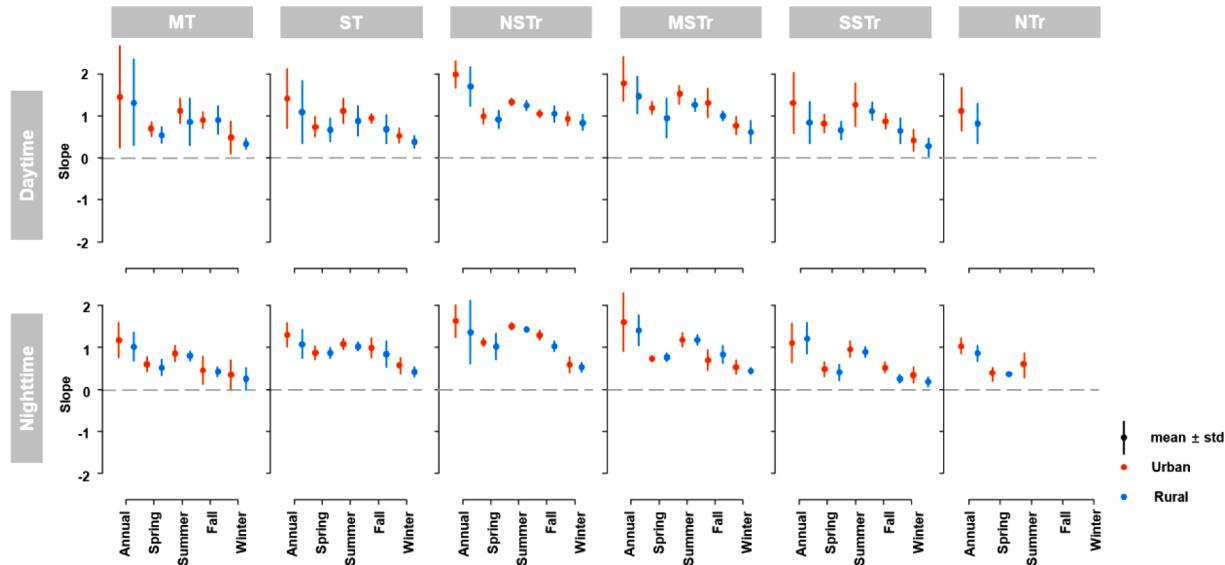


Fig. 5. The mean Sen's slope of the surface hot extreme intensity (Hxi) changes in various seasons from 2003 to 2020. The slope of the Hxi variation over urban areas is shown in red, while that over rural areas is shown in blue. The error bar is one standard deviation.

corresponding increase (all values significantly higher than zero in all climate zones, with a p-value < 0.05). Conversely, when SHX has solely affected rural environs, SUHI has demonstrated an opposing response (values significantly lower than zero in all climate zones). This distinct responsiveness of SUHI to urban and rural SHX, as mentioned earlier, has held true for both daytime and nighttime. However, when SHX has affected both urban areas and the surrounding rural regions, the responsiveness of SUHI has become notably intricate, precluding the determination of a dominant pattern (with no significant differences between the average δSUHII and zero in all seven climate zones). Seasonality in SUHI has garnered widespread recognition and extensive research, with seasonal variations in SUHI responsiveness to SHX observed across China. In comparison to spring and winter, the responsiveness of daytime/nighttime SUHI to independent urban and rural hot days/nights has been more pronounced in summer and fall.

The section primarily focuses on an in-depth exploration of the intricate responsiveness of the Urban Heat Island (SUHI) during compound hot day/night events (CHD/CHN), given the complexity that has been observed in their interactions. The absence of statistically significant differences in the average δSUHII relative to zero within each climate zone should not be misconstrued as an indication that SUHI remains unresponsive to surface hot extreme (SHX) episodes occurring during CHD and CHN. Fig. 6 has offered a comprehensive portrayal of the diverse SUHI responses to surface hot extremes in CHD and CHN, and how they have been regulated by the relative intensities of surface hot extremes in urban and rural areas. When urban surface hot extremes have exhibited greater intensity than their rural counterparts, both during the day and night, SUHI has exhibited a positive response (i.e., $\delta\text{SUHII} > 0$). Conversely, SUHI responsiveness has taken on an opposite direction ($\delta\text{SUHII} < 0$) when rural surface hot extremes have dominated in CHD or CHN scenarios. It is also worth noting that the greater the disparity in relative intensity between urban and rural surface hot extremes during CHD/CHN events (as observed in deviations from the 1:1 line in Fig. 6), the more pronounced the SUHI responsiveness, as indicated by the larger data points in Fig. 6. Additionally, when surface hot extremes have been isolated in either urban areas or rural surroundings with separate occurrences, significant correlations between hot extreme intensity (HXI) and SUHI responsiveness have been identified (as demonstrated in Figure S6). This observed responsive behavior is logically explained by the fact that SUHI represents the temperature difference between urban and rural areas, and the occurrence of SHX precisely corresponds to temperature anomalies.

3.3. Drivers of SUHI responsiveness to surface hot extreme

Nowadays, the biophysical mechanisms underlying the formation

and dynamics of SUHI have been relatively cemented (Li et al. 2019b; Manoli et al. 2019; Shen et al. 2023; Zhao et al. 2014). Nevertheless, the absence of a consensus persists when it comes to understanding the specific drivers that influence SUHI responses in various surface hot extreme (SHX) scenarios, largely due to the diverse climate conditions and local surface characteristics that come into play (He et al. 2021; Jiang et al. 2019; Li et al. 2015; Liao et al. 2021). In this study, we have delved into the examination of the magnitudes (as depicted in Figs. 7 and 8) and directions (illustrated in Figures S7 and S8) of the external drivers that impact SUHI responsiveness to surface hot extremes. This investigation has been conducted by employing advanced methods such as XGBoost and SHAP, allowing for a more comprehensive understanding of the complex interplay of these factors.

In comparison to non-surface hot extreme (NSHX) periods, the variations in surface evapotranspiration (δET , as depicted in Fig. 7) resulting from surface hot extreme (SHX) episodes have shown the most significant influence on daytime SUHI responsiveness (δSUHII). On hot days (i.e., IUHD, IRHD, and CHD), δET has had a positive impact on δSUHII , as shown in Figure S7. Conversely, increased daytime SUHI can be attributed to more negative disparities in rural surface evapotranspiration, generally falling below zero. This inconsistency primarily has arisen from the fact that δET , as used in this study, represents the variation in rural surface ET between NSHX conditions and SHX episodes. For Chinese cities, the average urban imperviousness (ISF) has also played a positive role in elevating the SUHI during hot days, as indicated in Figure S7. The higher the average urban imperviousness, the more pronounced this effect has become. Furthermore, variations in external climate forcings (e.g., downward radiation [δRAD], specific humidity [δSH], air temperature [δAT], wind speed [δWS], precipitation [δPRE], and soil moisture [δSM]) during hot days can also impact the responsiveness of daytime SUHI. These factors collectively contribute to the intricate dynamics of SUHI responsiveness, and their influence has been further explored in this study.

The nighttime hot extreme scenarios (IUHN, IRHN, and CHN) have significantly influenced urban-rural disparities in surface albedo (δABD , average SHAP value = 0.28) and mean imperviousness (ISF in Fig. 9, average SHAP value = 0.23) regarding nighttime SUHI responsiveness. This is due to the fact that nighttime SUHI primarily results from the release of excessive heat stored in urban areas during the night. Reduced urban surface albedo and increased impervious surface fraction (ISF) contribute to greater heat storage within urban surfaces during hot nights. Urban morphology has also played a role in shaping the sensitivity of SUHI to surface hot extremes on hot nights, as seen in the effects of built-up area (AREA, average SHAP value = 0.07) and the perimeter-area ratio (PAR, average SHAP value = 0.10). However, the impact of AREA and PAR on SUHI responsiveness varies across different surface

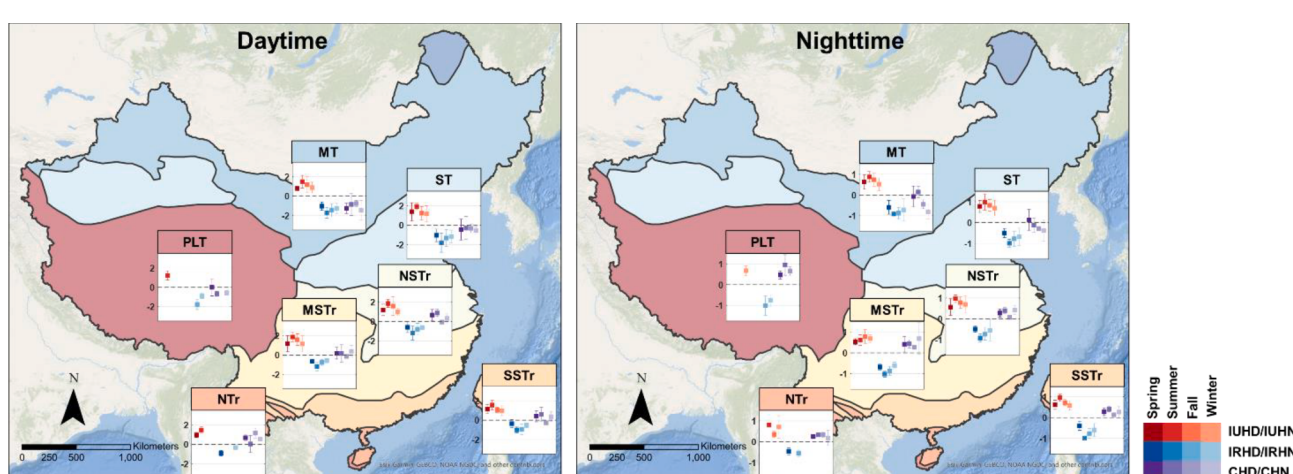


Fig. 6. The various SUHI responsiveness to surface hot extreme across climate zones in the daytime and nighttime.

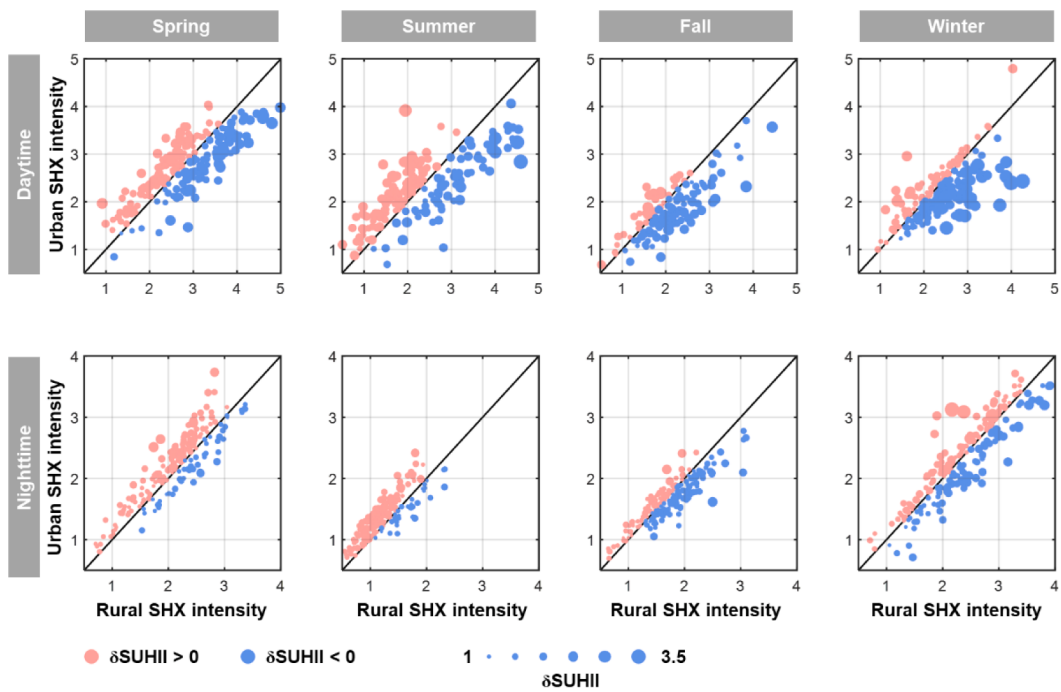


Fig. 7. Relationship between SUHI responsiveness with urban and rural surface hot extreme intensity in the daytime and nighttime across seasons.

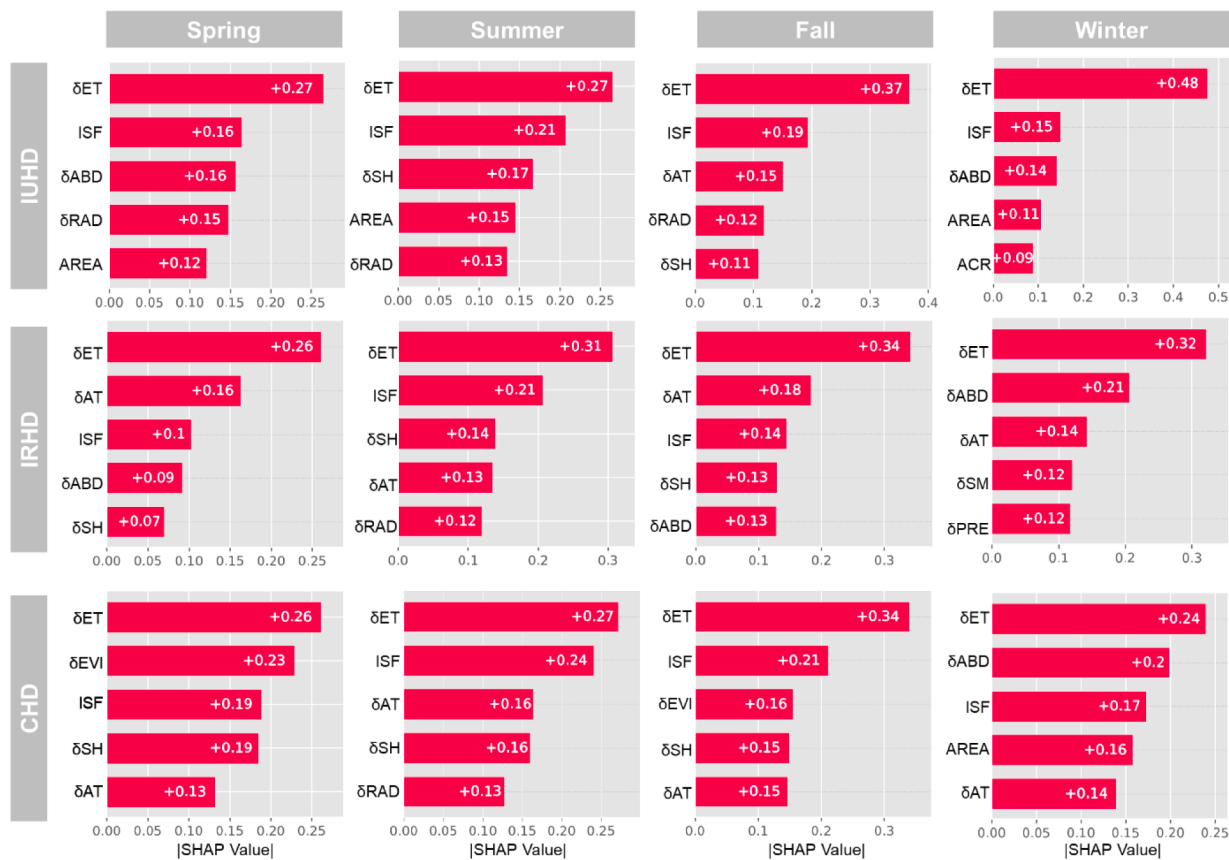


Fig. 8. Relative importance (measured by mean absolute SHAP values) of drivers of SUHI responsiveness to surface hot extremes in various hot days.

hot extreme scenarios. In cases where surface hot extremes have been confined to urban areas (UHN), urban clusters with a smaller PAR experience more significant SUHI intensification due to their compact form, which restricts the dissipation of excess heat into rural

surroundings. Similarly, during IRHN scenarios, the compact urban form has provided protection against rural hot extremes, establishing a positive correlation between δSUHII and PAR. The relationship between AREA and δSUHII has been varied and does not follow a consistent

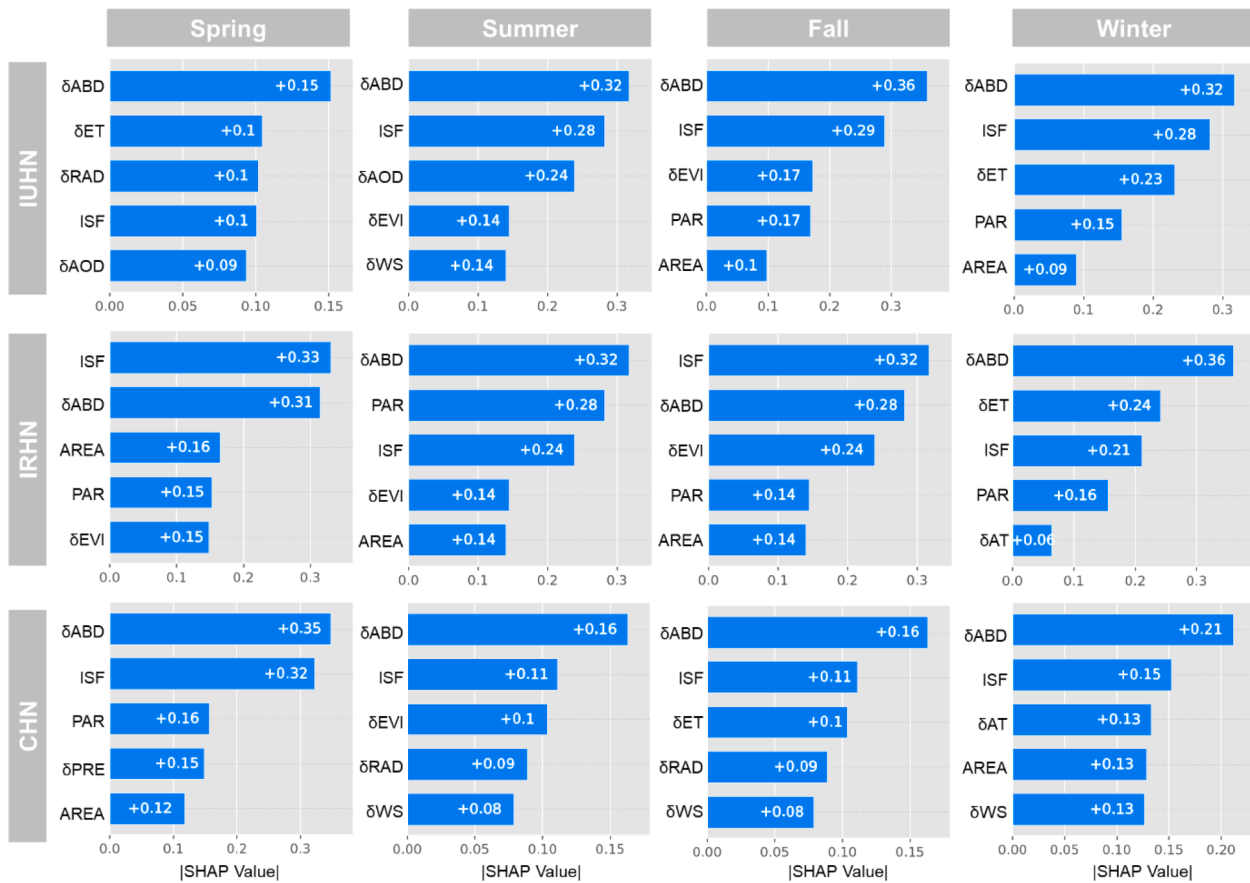


Fig. 9. Relative importance (measured by mean absolute SHAP values) of drivers of SUHI responsiveness to surface hot extreme in various hot nights.

pattern, as evident in Figure S8. Moreover, nighttime δSUHII , closely linked to the energy dynamics of nighttime SUHI, remains minimally affected by external climate conditions, such as δAT (temperature) and δPRE (precipitation).

4. Discussion

4.1. Enhanced surface hot extremes over Chinese urban clusters

In the present Anthropocene era, the combined impact of urbanization within the context of global warming has frequently led to an increased frequency of extreme events, notably surface hot extreme episodes. This is especially relevant for densely populated and rapidly urbanizing countries like China. Understanding these dynamics is both critical and imperative. The presence of the urban heat island (UHI) effect has exacerbated the impact of surface hot extremes on urban regions, resulting in significant damages and costs. Several studies have investigated the spatial patterns and temporal variations of hot extremes across China (Liao et al. 2021; Lu et al. 2016; Shi et al. 2021b). However, the majority of these studies have been based on spatially sparse air temperature (AT) observations or gridded reanalysis datasets. They have not comprehensively assessed changes in surface hot extremes within urban areas or explored the variations in SHX events between urban and rural regions.

Based on long-term seamless LST observations, our study has revealed an evident increase in the frequency, duration, and intensity of surface hot extremes across urban clusters and rural areas in China. Notably, both urban areas and the surrounding rural regions have witnessed more intense daytime hot extremes (DUHX and DRHX) in northern China, particularly in northeastern regions (as depicted in Fig. 2), when compared to the southern regions. In the higher latitudes

of the north, rural areas have experienced more intense surface hot extremes than urban areas, with differences in heat intensity of up to approximately 5°C between rural and urban locations. During nighttime, no noticeable disparities in hot extreme intensities have existed between urban and rural areas. Urban clusters located in mid-latitudinal regions, particularly in the middle and lower reaches of the Yangtze River, have also encountered more intense surface hot extreme episodes, akin to the conditions in northern high latitudes, with an annual heat intensity index (HIX) of approximately 20°C. Furthermore, the duration (HxD in Figure S2), frequency (HxF in Figure S3), and intensity (HXI in Fig. 3) of surface hot extremes have all displayed more significant increases within urban areas, both during the daytime and nighttime. This suggests that without immediate mitigation of climate change, Chinese urban clusters are poised to experience even more severe, prolonged, and frequent surface hot extremes in the future, particularly during the summer (Liao et al. 2021; Luo and Lau 2017; Shi et al. 2021b). Our findings are consistent with previous research based on air temperature observations, reinforcing the idea that urbanization exacerbates record-breaking daytime and nighttime extreme heat events (Luo et al. 2022; Shi et al. 2021b).

4.2. Dependencies of SUHI responses to SHX on the relative intensity of urban-rural SHX

In the late 21st century, hot extremes are projected to have increased frequency, longer durations, and larger spatial coverage due to global warming (Easterling et al. 2000; IPCC WG II 2022; Liao et al. 2021; Meehl and Tebaldi 2004; Mishra et al. 2015). Even in conditions with no surface hot extremes (NSHX), the urban surface commonly maintains higher temperatures than its rural counterpart due to the UHI effect. Consequently, it becomes imperative to investigate whether there is a

positive or synergistic relationship between UHI and SHX (He et al. 2021; Rogers et al. 2019; Ward et al. 2016; Zhao et al. 2018). While a positive association between UHI and SHX has been observed in specific regions (He et al. 2021; Jiang et al. 2019; Li and Bou-Zeid 2013; Miao et al. 2022), varied UHI responses during SHX episodes have been documented in urban clusters characterized by diverse local climates, physical features, and socioeconomic conditions (Fenner et al. 2019; Li et al. 2015; Mohammad Harmay and Choi 2022; Zhao et al. 2018). Recent studies on SUHI's responsiveness to SHX have primarily focused on specific climates and relied on air temperature (AT) observations to identify surface hot extremes. Cross-climate investigations have been limited to a few major cities due to the challenges of collecting high-quality in-situ AT data or gridded datasets with urban signals (Li and Bou-Zeid 2013; Ward et al. 2016; Zhao et al. 2018). Consequently, spatial and temporal patterns of SHX events detected through land surface temperature (LST) observations within various climate contexts have not been thoroughly explored, leaving uncertainty in how SUHI responds to SHX. Furthermore, investigating potential synergies between SUHI and SHX is crucial for a better understanding of future changes in the urban thermal environment, resulting from the intensified SHX in the combined context of urbanization and global warming (Chen and Zhang 2018; Founda and Santamouris 2017; He et al. 2021; Huang et al. 2019; Mentaschi et al. 2022; Scott et al. 2018; Wang and Li 2021). The concept of urban sustainability may face more significant challenges than the sum of the risks associated with SHX and SUHI if synergistic interactions between them exist (He et al. 2022; He et al. 2021; Masson et al. 2020).

This study has revealed divergent responses of SUHI to SHX episodes that occur in different spatial extents, namely urban areas or rural surroundings, during hot days and nights. As depicted in Fig. 5, when SHX episodes have exclusively taken place in urban areas (i.e., IUHD and IUHN), both daytime and nighttime SUHI have exhibited increased responses to surface hot extremes. Conversely, when SHX has exclusively occurred in rural areas (i.e., IRHD and IRHN), an inverse responsiveness of SUHI to SHX has been observed. Seasonal variations have been also evident in this SUHI responsiveness. When surface hot extremes have occurred solely in urban areas (i.e., during IUHD or IUHN), daytime and nighttime SUHI have experienced more pronounced elevations in summer and fall compared to spring and winter. Even when SUHI responsiveness has been negative ($\delta\text{SUHII} < 0$), it has remained more significant during summer and fall if SHX episodes exclusively transpire in rural areas. Given the significant correlations between HXI and δSUHII that we have discovered, the seasonal differences in SUHI responsiveness to HX are explicable. The HX events have been identified through satellite LST observations specifically representing LST anomalies in urban and rural areas. As a combined output of urban and rural LST, SUHI has responded accordingly to urban and rural LST anomalies in an anticipated manner (Founda and Santamouris 2017; Miao et al. 2022; Oke 1982; Voogt and Oke 2003). SUHI exhibits a more pronounced positive or negative response to urban or rural surface heat extremes (SHX) during the summer season, as surface hot extremes have tended to be more intense in various climate zones during this period. However, when hot extremes have occurred in both urban and rural areas on the same day/night (CHD or CHN), the responsiveness of SUHI to hot extremes has become elusive and does not exhibit consistent enhancement or suppression. The relative intensity of SHX occurring simultaneously in both urban and rural areas—namely, which area produces stronger LST anomalies—determines the strength and direction of SUHI responsiveness, as demonstrated in Fig. 6.

4.3. Different drivers behind the responses of daytime and nighttime SUHI to SHX

The overarching surface energy balance (SEB), encompassing factors such as energy input, loss, generation, and storage in the built environment, forms the foundational basis for SUHI (Founda and

Santamouris 2017; Li et al. 2015; Oke 1982; Shen et al. 2023). Daytime SUHI is primarily influenced by disparities in evaporative and convective cooling between urban and rural areas, while differences in anthropogenic heat release and heat storage are the key drivers of nighttime SUHI. Examining the components of the surface energy budget in both urban and rural areas during SHX and NSHX periods can provide valuable insights into SUHI responsiveness. However, quantifying each component of the surface energy budget over an extensive temporal and spatial scale is nearly impractical due to limitations in surface heat flux observations. Consequently, we have compiled a comprehensive list of potential drivers of SUHI responsiveness to SHX (as detailed in Table S1) from existing studies focused on SUHI-SHX relationships. The significance and underlying mechanisms of these potential drivers in influencing SUHI responsiveness have been explored using the explainable machine learning framework (i.e., XGBoost + SHAP).

Our results have demonstrated that the primary driver of daytime SUHI responsiveness to SHX is the differences in surface evapotranspiration (δET) during surface hot extremes compared to NSHX conditions. Urban imperviousness (ISF) and the urban-rural albedo disparities (δABD) have also significantly impacted how responsive SUHI is to HSX during the daytime. These three factors considerably modulate the partition of available surface energy in urban and rural areas during surface hot extremes. The latent heat flux (surface evapotranspiration) has dramatically risen during surface hot extremes in both urban and rural areas, according to current knowledge (Benson and Dirmeyer 2021; Benz et al. 2021; He et al. 2020; Li et al. 2015; Mohammad Harmay and Choi 2022; Wang and Li 2021; Zhao et al. 2018). The increase in latent heat flux within rural backgrounds, slightly greater due to the limited surface water supply in urban areas, has directly impacted the SUHI responsive behavior during surface hot extremes (He et al. 2020; Li et al. 2015; Mohammad Harmay and Choi 2022; Oke et al. 2017; Possega et al. 2022; Wang and Li 2021). Similar to δSUHII , δET operates within the urban-rural dichotomy, allowing alterations in urban and rural ET to induce bidirectional changes in δET . Consequently, the cascade effect in the urban-rural contrasts in LST and ET has resulted in bidirectional responsiveness in δSUHII (Founda and Santamouris 2017; Li and Bou-Zeid 2013; Li et al. 2015; Miao et al. 2022). During NSHX periods, sensible heat fluxes in urban areas have been consistently higher than in rural regions due to the lack of greenery and the use of impervious materials with lower albedo. Sensible heat flux has been greater in urban areas than in rural surroundings during surface hot extremes because SHX onsets have been typically characterized by constant stable weather conditions (e.g., less cloudiness, slower wind, more downward radiation, higher temperatures, and the like) (Founda and Santamouris 2017; Jiang et al. 2019; Li and Bou-Zeid 2013; Wang and Li 2019, 2021). The urban-rural disparities in surface albedo (δABD) as well as the average imperviousness of urban areas (ISF) have been critical factors in this process.

Similarly, because of lower albedo and higher imperviousness within built-up environments than in rural backgrounds, more energy has been stored within urban areas, dominating the responsiveness of nighttime SUHI to SHX (He et al. 2022; Jiang et al. 2019; Oke et al. 2017; Wang and Li 2019, 2021). Interestingly, this study has also revealed that urban morphology can significantly impact the nighttime responsiveness of SUHI. In the case of Chinese urban clusters, the influence of urban built-up area size on nighttime SUHI responsiveness to SHX has been bidirectional. In other words, larger urban clusters have not consistently exhibited enhanced SUHI during surface hot extremes (Li and Bou-Zeid 2013; Ward et al. 2016; Zhao et al. 2018). Furthermore, for individual urban hot nights (IUHN) and individual rural hot nights (IRHN), urban compactness has exerted a distinct influence on nighttime SUHI responsiveness. When SHXs have been confined within urban areas (during IUHN), urban clusters with a more compact shape (i.e., lower perimeter-area ratio [PAR]) have exhibited a stronger positive response of SUHI to surface hot extremes because they store more heat due to less

effective convective cooling (Oke et al. 2017; Ramamurthy and Bou-Zeid 2017; Wang and Li 2021; Wang et al. 2020). Conversely, less compact urban clusters have demonstrated stronger δ SUHII when surface hot extremes have been isolated from urban areas (during IRHN) because the looser shape has allowed for more effective urban-suburban heat exchange (He et al. 2022; Miao et al. 2022; Mohammad Harmay and Choi 2022; Oke et al. 2017; Wang and Li 2019; Wang et al. 2020).

4.4. Implications and limitations

In the context of urbanization and global change, cities are in urgent need of effective cooling strategies to shelter urban dwellers from potential UHI and heatwave synergies. This study provides evidence that heightened attention is warranted towards summer hot extremes. Beyond being a mere sum of UHI and SHX, the risks to the urban thermal environment during hot extremes are far more menacing. The potential jump of SUHI during SHX could pose a more substantial challenge to urban well-being and sustainability, particularly in light of the escalating frequency, duration, and intensity of SHX events (Huang et al. 2019; Liao et al. 2021; Mora et al. 2017; Nazarian et al. 2022; Qin et al. 2023; Romanello et al. 2021). Practices like the adaptation of green roofs (Georgescu, Morefield, Bierwagen, & Weaver, 2014; Zhang & He, 2021) and urban greening (Goodwin, Olazabal, Castro, & Pascual, 2023), as well as using white roofs that increase the reflection of incoming shortwave radiation (He et al. 2022; Ouyang et al., 2022) can be beneficial. The disparities in drivers affecting daytime and nighttime responsiveness to hot extremes underscore the need for meticulous consideration of synergies and trade-offs among various mitigation techniques. For instance, to ensure the cooling effectiveness of green roofs during SHX, maintaining high soil moisture levels through irrigation becomes essential (Gao et al. 2020; Grimmond 2007; Igun et al. 2023; Ngarambe et al. 2020). However, the impact of changes in surface albedo due to irrigation and greening on local surface temperatures (LST) remains unclear. Certain urban clusters may find the act of planting (in tropical urban clusters) or irrigating (in arid-climate urban clusters) impractical or economically unfeasible (Li et al. 2023; Manoli et al. 2019). For instance, in the case of most cities located in the mid-latitude or high-latitude regions of the Northern Hemisphere, urban forests are considered an ideal urban cooling practice due to their capacity to provide significant evaporative cooling (Paschalidis et al. 2021). However, in cities with a hot and humid climate, the cooling potential of forests tends to approach saturation (Manoli et al. 2020; Manoli et al. 2019).

However, limitations remain and further efforts are needed. Up to now, there is no universally accepted criterion for defining and identifying surface hot extremes, whether based on AT or LST (Easterling et al. 2000; Wu et al. 2021; You et al. 2017). The use of both absolute and relative threshold temperatures can lead to noticeable differences in the duration and intensity of identified hot extreme episodes (Easterling et al. 2000; Meehl and Tebaldi 2004; Perkins and Alexander 2013). Consequently, variations in the terminology employed to define surface hot extremes and the subsequent discrepancies in the observed responsive behavior of SUHI are expected (Cheng et al. 2023; Miao et al. 2022). Furthermore, explainable machine learning, mainly the XGBoost and SHAP, has constituted the primary methodology employed to investigate the underlying mechanisms of the responsiveness of SUHI to SHX in this study. While the powerful nonlinear modeling capability of XGBoost and the causal inference ability of SHAP have enabled existing ML-based frameworks to robustly attribute δ SUHII, it is worth noting that incorporating additional biophysical considerations, such as coupling with numerical models, in future attribution studies would enhance the robustness of the exploration of drivers behind δ SUHII. A more prospective solution involves integrating this framework with more advanced physically-based models to attain a deeper understanding of the underlying processes. Owing to constraints inherent in in-situ meteorological and energy flux observations, the present analysis of

driving factors can only be conducted relying on reanalyzed data. It must be acknowledged that this reliance on reanalysis information could introduce a level of uncertainty to the study, potentially diminishing the potential significance. Future efforts are expected to considerably improve our understanding of SUHI-SHX interactions by integrating more advanced urban modeling with broader energy flux observations (He et al. 2020; Li et al. 2015; Zhao et al. 2018).

5. Conclusion

Beating the adverse effects of extreme heat events within urban built-up contexts necessitates a comprehensive understanding of how the urban thermal environment responds to hot extremes. This study enlightens ongoing discussions on the responsiveness of daytime and nighttime SUHI (δ SUHII) to SHX. Over Chinese urban clusters, we have identified the spatiotemporal patterns of surface hot extremes and the responsiveness of daytime and nighttime SUHI to SHX in various scenarios based on the daily seamless LST observations. Geographically, northern Chinese urban clusters have exhibited heightened daytime and nighttime hot extreme intensity compared to their southern counterparts. Moreover, mid-latitude urban clusters have also experienced relatively stronger nighttime SHX. Temporally, regardless of the climatic context, Chinese urban clusters have consistently encountered more prolonged, frequent, and intense daytime and nighttime surface hot extremes during the summer and fall seasons. Our findings have revealed contrasting SUHI responsiveness to SHX across China. When SHX has solely impacted urban areas (IUHD and IUHN), both daytime and nighttime SUHI have demonstrated positive responsiveness (δ SUHII>0). Conversely, when surface hot extremes have been restrained to rural zones, SUHI has exhibited negative responsiveness (δ SUHII<0). Notably, the relative intensity of urban and rural SHX has been positively correlated with δ SUHII. Furthermore, employing an explainable machine learning framework, we have illustrated that the responsiveness of daytime and nighttime SUHI to SHX have been associated with the variations in surface evaporative cooling-related factors (primarily δ ET during the daytime), and surface heat storage-related factors (primarily δ ABD and ISF during the nighttime) during SHX episodes, respectively. Overall, our findings provide fresh evidence of SUHI responses to hot extremes (δ SUHII) across diverse climates. The investigation into underlying driving forces also contributes to urban cooling strategies aimed at mitigating potential synergies between SUHI and surface hot extremes. In the future, the exploration of deeper biophysical mechanisms of SUHI responsiveness can be enhanced through the integration of advanced urban models and field observations.

Author contributions

S.Z. designed the research; C.Y. and S.Z performed research, analyzed data and wrote the paper.

Declaration of Competing Interest

The authors declare no competing interests.

Data availability

Data will be made available on request.

Acknowledgments

This study was supported by the National Key R&D Plan of China Grant (2023YFF1304602) and the National Natural Science Foundation of China Grant (42071120).

Supplementary materials

Supplementary material associated with this article can be found, in the online version, at doi:10.1016/j.scs.2023.105093.

References

- Amani-Beni, M., Chen, Y., Vasileva, M., Zhang, B., & Xie, G. D. (2022). Quantitative spatial relationships between air and surface temperature, a proxy for microclimate studies in fine-scale intra-urban areas? *Sustainable Cities and Society*, 77, Article 103584.
- Anderson, B. G., & Bell, M. L. (2009). Weather-related mortality: How heat, cold, and heat waves affect mortality in the United States. *Epidemiology (Cambridge, Mass.)*, 20, 205.
- Angel, S., Parent, J., Civco, D. L., & Blei, A. M. (2011). *Making room for a planet of cities*. MA: Lincoln Institute of Land Policy Cambridge.
- Benson, D. O., & Dirmeyer, P. A. (2021). Characterizing the Relationship between Temperature and Soil Moisture Extremes and Their Role in the Exacerbation of Heat Waves over the Contiguous United States. *Journal of Climate*, 34, 2175–2187.
- Benz, S. A., Davis, S. J., & Burney, J. A. (2021). Drivers and projections of global surface temperature anomalies at the local scale. *Environmental Research Letters*, 16, Article 064093.
- Berdugo, M., Gaitán, J. J., Delgado-Baquerizo, M., Crowther, T. W., & Dakos, V. (2022). Prevalence and drivers of abrupt vegetation shifts in global drylands. *Proceedings of the National Academy of Sciences*, 119.
- Bi, X., Wu, C., Wang, Y., Li, J., Wang, C., Hahs, A., et al. (2023). Changes in the associations between heatwaves and human mortality during two extreme hot summers in Shanghai, China. *Sustainable Cities and Society*, 95, Article 104581.
- Chen, T., & Guestrin, C. (2016). Xgboost: A scalable tree boosting system. In (pp. 785–794).
- Chen, T., & Guestrin, C. Xgboost: A scalable tree boosting system. In (pp. 785–794).
- Chen, Y., & Zhang, N. (2018). Urban Heat Island Mitigation Effectiveness under Extreme Heat Conditions in the Suzhou–Wuxi–Changzhou Metropolitan Area, China. *Journal of Applied Meteorology and Climatology*, 57, 235–253.
- Chen, Y., Wang, Y., Zhou, D., Gu, Z., & Meng, X. (2022). Summer urban heat island mitigation strategy development for high-anthropogenic-heat-emission blocks. *Sustainable Cities and Society*, 87, Article 104197.
- Cheng, Q., Jin, H., & Ren, Y. (2023). Compound daytime and nighttime heatwaves for air and surface temperature based on relative and absolute threshold dynamic classified in Southwest China, 1980–2019. *Sustainable Cities and Society*, 91, Article 104433.
- China National Institute of Standardization, C.M.A. (1998). *Names and codes for climate regionalization in china*. Standards Press of China.
- Dong, Z., Wang, L., Sun, Y., Hu, T., Limsakul, A., Singhru, P., et al. (2021). Heatwaves in Southeast Asia and Their Changes in a Warmer World. *Earth's Future*, 9.
- Easterling, D. R., Meehl, G. A., Parmesan, C., Changnon, S. A., Karl, T. R., & Mearns, L. O. (2000). Climate Extremes: Observations, Modeling, and Impacts. *Science (New York, N.Y.)*, 289, 2068–2074.
- Fenner, D., Holtmann, A., Meier, F., Langer, I., & Scherer, D. (2019). Contrasting changes of urban heat island intensity during hot weather episodes. *Environmental Research Letters*, 14, Article 124013.
- Founda, D., & Santamouris, M. (2017). Synergies between Urban Heat Island and Heat Waves in Athens (Greece), during an extremely hot summer (2012). *Scientific Reports*, 7, 1–11.
- Gao, K., Santamouris, M., & Feng, J. (2020). On the cooling potential of irrigation to mitigate urban heat island. *Science of the Total Environment*, 740, Article 139754.
- Gao, S., Chen, Y., Li, K., He, B., Hou, P., & Guo, Z. (2023). Frequent heatwaves limit the indirect growth effect of urban vegetation in China. *Sustainable Cities and Society*, 96, Article 104662.
- Georgescu, M., Morefield, P. E., Bierwagen, B. G., & Weaver, C. P. (2014). Urban adaptation can roll back warming of emerging megapolitan regions. *Proceedings of the National Academy of Sciences*, 111(8), 2909–2914.
- Good, E. J., Ghent, D. J., Bulgin, C. E., & Remedios, J. J. (2017). A spatiotemporal analysis of the relationship between near-surface air temperature and satellite land surface temperatures using 17 years of data from the ATSR series. *Journal of Geophysical Research: Atmospheres*, 122, 9185–9210.
- Goodwin, S., Olazabal, M., Castro, A. J., & Pascual, U. (2023). Global mapping of urban nature-based solutions for climate change adaptation. *Nature Sustainability*, 1–12.
- Grimmond, S. (2007). Urbanization and global environmental change: Local effects of urban warming. *The Geographical Journal*, 173, 83–88.
- He, X., Wang, J., Feng, J., Yan, Z., Miao, S., Zhang, Y., et al. (2020). Observational and modeling study of interactions between urban heat island and heatwave in Beijing. *Journal of Cleaner Production*, 247, Article 119169.
- He, B. J., Wang, J., Liu, H., & Ulpiani, G. (2021). Localized synergies between heat waves and urban heat islands: Implications on human thermal comfort and urban heat management. *Environ Res*, 193, Article 110584.
- He, B. J., Wang, J., Zhu, J., & Qi, J. (2022). Beating the urban heat: Situation, background, impacts and the way forward in China. *Renewable and Sustainable Energy Reviews*, 161, Article 112350.
- Hsu, A., Sheriff, G., Chakraborty, T., & Manya, D. (2021). Disproportionate exposure to urban heat island intensity across major US cities. *Nature Communications*, 12.
- Huang, K., Li, X., Liu, X., & Seto, K. C. (2019). Projecting global urban land expansion and heat island intensification through 2050. *Environmental Research Letters*, 14, Article 114037.
- Igun, E., Xu, X., Shi, Z., & Jia, G. (2023). Enhanced nighttime heatwaves over African urban clusters. *Environmental Research Letters*, 18, Article 014001.
- IPCC WG II, I. W. G. I. (2022). *Climate change 2022: Impacts, adaptation and vulnerability*. IPCC.
- Jiang, S., Lee, X., Wang, J., & Wang, K. (2019). Amplified Urban Heat Islands during Heat Wave Periods. *Journal of Geophysical Research: Atmospheres*, 124, 7797–7812.
- Jin, K., Wang, F., & Wang, S. (2020). Assessing the spatiotemporal variation in anthropogenic heat and its impact on the surface thermal environment over global land areas. *Sustainable Cities and Society*, 63, Article 102488.
- Kim, Y., & Kim, Y. (2022). Explainable heat-related mortality with random forest and SHapley Additive exPlanations (SHAP) models. *Sustainable Cities and Society*, 79.
- Li, D., & Bou-Zeid, E. (2013). Synergistic Interactions between Urban Heat Islands and Heat Waves: The Impact in Cities Is Larger than the Sum of Its Parts. *Journal of Applied Meteorology and Climatology*, 52, 2051–2064.
- Li, D., Sun, T., Liu, M., Yang, L., Wang, L., & Gao, Z. (2015). Contrasting responses of urban and rural surface energy budgets to heat waves explain synergies between urban heat islands and heat waves. *Environmental Research Letters*, 10, Article 054009.
- Li, D., Sun, T., Liu, M., Wang, L., & Gao, Z. (2016). Changes in Wind Speed under Heat Waves Enhance Urban Heat Islands in the Beijing Metropolitan Area. *Journal of Applied Meteorology and Climatology*, 55, 2369–2375.
- Li, B., Rodell, M., Kumar, S., Beaudoin, H. K., Getirana, A., & Zaitchik, B. F. (2019a). Global GRACE data assimilation for groundwater and drought monitoring: Advances and challenges. *Water Resources Research*, 55, 7564–7586.
- Li, D., Liao, W., Rigden, A. J., Liu, X., Wang, D., Malyshev, S., et al. (2019b). Urban heat island: Aerodynamics or imperviousness? *Science Advances*, 5, eaau4299.
- Li, Y., Li, Z. L., Wu, H., Zhou, C., Liu, X., Leng, P., et al. (2023). Biophysical impacts of earth greening can substantially mitigate regional land surface temperature warming. *Nature Communications*, 14.
- Liao, W., Li, D., Malyshev, S., Shevliakova, E., Zhang, H., & Liu, X. (2021). Amplified Increases of Compound Hot Extremes Over Urban Land in China. *Geophysical Research Letters*, 48.
- Lu, C., Sun, Y., Wan, H., Zhang, X., & Yin, H. (2016). Anthropogenic influence on the frequency of extreme temperatures in China. *Geophysical Research Letters*, 43, 6511–6518.
- Lundberg, S. M., & Lee, S. I. (2017). A unified approach to interpreting model predictions. *Advances in neural information processing systems* (p. 30).
- Lundberg, S. M., Erion, G., Chen, H., DeGrave, A.,普鲁特金, J. M., Nair, B., et al. (2020). From local explanations to global understanding with explainable AI for trees. *Nature Machine Intelligence*, 2, 56–67.
- Luo, M., & Lau, N. C. (2017). Heat Waves in Southern China: Synoptic Behavior, Long-Term Change, and Urbanization Effects. *Journal of Climate*, 30, 703–720.
- Luo, M., Lau, G., Liu, Z., Wu, S., & Wang, X. (2022). An observational investigation of spatiotemporally contiguous heatwaves in China from a 3D perspective. *Geophysical Research Letters*.
- Mann, H. B. (1945). Nonparametric Tests Against Trend. *Econometrica : journal of the Econometric Society*, 13, 245–259.
- Manoli, G., Fatichi, S., Schläpfer, M., Yu, K., Crowther, T. W., Meili, N., et al. (2019). Magnitude of urban heat islands largely explained by climate and population. *Nature*, 573, 55–60.
- Manoli, G., Fatichi, S., Schläpfer, M., Yu, K., Crowther, T. W., Meili, N., et al. (2020). Reply to Martilli et al. (2020): Summer average urban-rural surface temperature differences do not indicate the need for urban heat reduction. OSF Preprints.
- Masson, V., Lemonsu, A., Hidalgo, J., & Voogt, J. (2020). Urban Climates and Climate Change. *Annual Review of Environment and Resources*, 45, 411–444.
- Meehl, G. A., & Tebaldi, C. (2004). More intense, more frequent, and longer lasting heat waves in the 21st century. *Science (New York, N.Y.)*, 305, 994–997.
- Melaas, E. K., Wang, J. A., Miller, D. L., & Friedl, M. A. (2016). Interactions between urban vegetation and surface urban heat islands: A case study in the Boston metropolitan region. *Environmental Research Letters*, 11, Article 054020.
- Mentaschi, L., Duveiller, G., Julian, G., Corbane, C., Pesaresi, M., Maes, J., et al. (2022). Global long-term mapping of surface temperature shows intensified intra-city urban heat island extremes. *Global Environmental Change*, 72, Article 102441.
- Miao, S., Zhan, W., Lai, J., Li, L., Du, H., Wang, C., et al. (2022). Heat wave-induced augmentation of surface urban heat islands strongly regulated by rural background. *Sustainable Cities and Society*, 82, Article 103874.
- Mishra, V., Ganguly, A. R., Nijssen, B., & Lettenmaier, D. P. (2015). Changes in observed climate extremes in global urban areas. *Environmental Research Letters*, 10, Article 024005.
- Mohammad Harmay, N. S., & Choi, M. (2022). Effects of heat waves on urban warming across different urban morphologies and climate zones. *Building and Environment*, 209, Article 108677.
- Mora, C., Dousset, B., Caldwell, I. R., Powell, F. E., Geronimo, R. C., & Bielecki, C. R. (2017). Global risk of deadly heat. *Nature Climate Change*, 7, 501–506.
- Nangombe, S., Zhou, T., Zhang, W., Wu, B., Hu, S., Zou, L., et al. (2018). Record-breaking climate extremes in Africa under stabilized 1.5 C and 2 C global warming scenarios. *Nature Climate Change*, 8, 375–380.
- Nazarian, N., Krähenhoff, E. S., Bechtel, B., Hondula, D. M., Paolini, R., Vanos, J., et al. (2022). Integrated Assessment of Urban Overheating Impacts on Human Life. *Earth's Future*, 10.
- Ngarambe, J., Nganyiyimana, J., Kim, I., Santamouris, M., & Yun, G. Y. (2020). Synergies between urban heat island and heat waves in Seoul: The role of wind speed and land use characteristics. *PLoS One*, 15, Article e0243571.
- Oke, T. R., Mills, G., Christen, A., & Voogt, J. A. (2017). *Urban climates*. Cambridge University Press.

- Oke, T. R. (1973). City size and the urban heat island. *Atmospheric Environment* (1967), 7, 769–779.
- Oke, T. R. (1982). The energetic basis of the urban heat island. *Quarterly Journal of the Royal Meteorological Society*, 108, 1–24.
- Oukawa, G. Y., Kreel, P., & Targino, A. C. (2022). Fine-scale modeling of the urban heat island: A comparison of multiple linear regression and random forest approaches. *Science of the Total Environment*, 815, Article 152836.
- Ouyang, Z., Sciusco, P., Jiao, T., Feron, S., Lei, C., Li, F., & Chen, J. (2022). Albedo changes caused by future urbanization contribute to global warming. *Nature Communications*, 13(1), 3800.
- Paschalidis, A., Chakraborty, T., Fatichi, S., Meili, N., & Manoli, G. (2021). Urban Forests as Main Regulator of the Evaporative Cooling Effect in Cities. *AGU Advances*, 2.
- Pedregosa, F., Varoquaux, G., Gramfort, A., Michel, V., Thirion, B., Grisel, O., et al. (2011). Scikit-learn: Machine learning in Python. *Journal of Machine Learning Research*, 12, 2825–2830.
- Perkins, S. E., & Alexander, L. V. (2013). On the Measurement of Heat Waves. *Journal of Climate*, 26, 4500–4517.
- Possega, M., Aragão, L., Ruggieri, P., Santo, M. A., & Di Sabatino, S. (2022). Observational evidence of intensified nocturnal urban heat island during heatwaves in European cities. *Environmental Research Letters*, 17, Article 124013.
- Qin, Y., Liao, W., & Li, D. (2023). Attributing the Urban-Rural Contrast of Heat Stress Simulated by a Global Model. *Journal of Climate*, 36, 1805–1822.
- Ramamurthy, P., & Bou-Zeid, E. (2017). Heatwaves and urban heat islands: A comparative analysis of multiple cities. *Journal of Geophysical Research: Atmospheres*, 122, 168–178.
- Rogers, C. D. W., Gallant, A. J. E., & Tapper, N. J. (2019). Is the urban heat island exacerbated during heatwaves in southern Australian cities? *Theoretical and Applied Climatology*, 137, 441–457.
- Romanello, M., McGushin, A., Di Napoli, C., Drummond, P., Hughes, N., Jamart, L., et al. (2021). The 2021 report of the Lancet Countdown on health and climate change: Code red for a healthy future. *The Lancet*, 398, 1619–1662.
- Rosenfeld, H. D., Rybski, D., Andrade, J. S., Batty, M., Stanley, H. E., & Makse, H. A. (2008). Laws of population growth. *Proceedings of the National Academy of Sciences*, 105, 18702–18707.
- Rydin, Y., Bleahu, A., Davies, M., Dávila, J. D., Friel, S., De Grandis, G., et al. (2012). Shaping cities for health: Complexity and the planning of urban environments in the 21st century. *The Lancet*, 379, 2079–2108.
- Scott, A. A., Waugh, D. W., & Zaitchik, B. F. (2018). Reduced Urban Heat Island intensity under warmer conditions. *Environmental Research Letters*, 13, Article 064003.
- Sen, P. K. (1968). Estimates of the regression coefficient based on Kendall's tau. *Journal of the American statistical association*, 63, 1379–1389.
- Shen, P., Zhao, S., & Ma, Y. (2021). Perturbation of Urbanization to Earth's Surface Energy Balance. *Journal of Geophysical Research: Atmospheres*, 126.
- Shen, P., Zhao, S., Ma, Y., & Liu, S. (2023). Urbanization-induced Earth's surface energy alteration and warming: A global spatiotemporal analysis. *Remote Sensing of Environment*, 284, Article 113361.
- Shi, Z., Jia, G., Zhou, Y., Xu, X., & Jiang, Y. (2021a). Amplified intensity and duration of heatwaves by concurrent droughts in China. *Atmospheric Research*, 261, Article 105743.
- Shi, Z., Xu, X., & Jia, G. (2021b). Urbanization Magnified Nighttime Heat Waves in China. *Geophysical Research Letters*, 48.
- Sun, Y., Zhang, X., Zwiers, F. W., Song, L., Wan, H., Hu, T., et al. (2014). Rapid increase in the risk of extreme summer heat in Eastern China. *Nature Climate Change*, 4, 1082–1085.
- Tan, J., Zheng, Y., Tang, X., Guo, C., Li, L., Song, G., et al. (2010). The urban heat island and its impact on heat waves and human health in Shanghai. *International Journal of Biometeorology*, 54, 75–84.
- United Nations, U. (2018). World urbanization prospects 2018. United Nations Department for Economic and Social Affairs.
- Venter, Z., Chakraborty, T., & Lee, X. (2021). Crowdsourced air temperatures contrast satellite measures of the urban heat island and its mechanisms. *Science Advances*, 7.
- Voogt, J., & Oke, T. (2003). Thermal Remote Sensing of Urban Climates. *Remote Sensing of Environment*, 86, 370–384.
- Wang, L., & Li, D. (2019). Modulation of the urban boundary-layer heat budget by a heatwave. *Quarterly Journal of the Royal Meteorological Society*, 145, 1814–1831.
- Wang, L., & Li, D. (2021). Urban Heat Islands during Heat Waves: A Comparative Study between Boston and Phoenix. *Journal of Applied Meteorology and Climatology*, 60, 621–641.
- Wang, C., Zhang, Z., Zhou, M., Zhang, L., Yin, P., Ye, W., et al. (2017). Nonlinear relationship between extreme temperature and mortality in different temperature zones: A systematic study of 122 communities across the mainland of China. *Science of the Total Environment*, 586, 96–106.
- Wang, L., Li, D., Zhang, N., Sun, J., & Guo, W. (2020). Surface Urban Heat and Cool Islands and Their Drivers: An Observational Study in Nanjing, China. *Journal of Applied Meteorology and Climatology*, 59, 1987–2000.
- Ward, K., Lauf, S., Kleinschmit, B., & Endlicher, W. (2016). Heat waves and urban heat islands in Europe: A review of relevant drivers. *Science of the Total Environment*, 569–570, 527–539.
- Wei, C., Chen, W., Lu, Y., Blaschke, T., Peng, J., & Xue, D. (2021). Synergies between Urban Heat Island and Urban Heat Wave Effects in 9 Global Mega-Regions from 2003 to 2020. *Remote Sensing*, 14, 70.
- World Meteorological Organization. (1989). Calculation of monthly and annual 30-year standard normals. In , 10. WCDP. WMO-TD 341.
- World Meteorological Organization. (2017). *WMO guidelines on the calculation of climate normals*. GEneva, Switzerland: World Meteorological Organization.
- Wu, X., Wang, L., Yao, R., Luo, M., & Li, X. (2021). Identifying the dominant driving factors of heat waves in the North China Plain. *Atmospheric Research*, 252, Article 105458.
- Yang, J., & Huang, X. (2021). The 30 m annual land cover dataset and its dynamics in China from 1990 to 2019. *Earth Syst. Sci. Data*, 13, 3907–3925.
- Yin, J., Gentile, P., Slater, L., Gu, L., Pokhrel, Y., Hanasaki, N., et al. (2023). Future socio-ecosystem productivity threatened by compound drought–heatwave events. *Nature Sustainability*.
- You, Q., Jiang, Z., Kong, L., Wu, Z., Bao, Y., Kang, S., et al. (2017). A comparison of heat wave climatologies and trends in China based on multiple definitions. *Climate Dynamics*, 48, 3975–3989.
- Zhang, G., & He, B.-J. (2021). Towards green roof implementation: Drivers, motivations, barriers and recommendations. *Urban Forestry & Urban Greening*, 58, 126992.
- Zhang, B., & Zhu, G. (1959). *Climate regionalization in china (first draft)*. Beijing: Science Press.
- Zhang, T., Zhou, Y., Zhu, Z., Li, X., & Asrar, G. R. (2022). A global seamless 1 km resolution daily land surface temperature dataset (2003–2020). *Earth System Science Data*, 14, 651–664.
- Zhao, L., Lee, X., Smith, R. B., & Oleson, K. (2014). Strong contributions of local background climate to urban heat islands. *Nature*, 511, 216–219.
- Zhao, S., Liu, S., & Zhou, D. (2016). Prevalent vegetation growth enhancement in urban environment. *Proceedings of the National Academy of Sciences*, 113, 6313.
- Zhao, L., Oppenheimer, M., Zhu, Q., Baldwin, J. W., Ebi, K. L., Bou-Zeid, E., et al. (2018). Interactions between urban heat islands and heat waves. *Environmental Research Letters*, 13, Article 034003.
- Zhao, M., Cheng, C., Zhou, Y., Li, X., Shen, S., & Song, C. (2022). A global dataset of annual urban extents (1992–2020) from harmonized nighttime lights. *Earth System Science Data*, 14, 517–534.
- Zheng, J. Y., Yin, Y., & Li, B. (2010). A new scheme for climate regionalization in China. *Acta Geographica Sinica*, 65, 3–12.
- Zheng, Z., Zhao, L., & Oleson, K. W. (2021). Large model structural uncertainty in global projections of urban heat waves. *Nature Communications*, 12.
- Zhou, D., Zhao, S., Liu, S., Zhang, L., & Zhu, C. (2014). Surface urban heat island in China's 32 major cities: Spatial patterns and drivers. *Remote Sensing of Environment*, 152, 51–61.
- Zhou, D., Zhang, L., Li, D., Huang, D., & Zhu, C. (2016). Climate–vegetation control on the diurnal and seasonal variations of surface urban heat islands in China. *Environmental Research Letters*, 11, Article 074009.
- Zhou, L., Hu, F., Wang, B., Wei, C., Sun, D., & Wang, S. (2022). Relationship between urban landscape structure and land surface temperature: Spatial hierarchy and interaction effects. *Sustainable Cities and Society*, 80.